Editors' Suggestion

Superconducting Qubit Based on Twisted Cuprate Van der Waals Heterostructures

Valentina Brosco,[1,2,*] Giuseppe Serpico,[3,4] Valerii Vinokur,[5,6] Nicola Poccia,[7] and Uri Vool[3,†]
[1]Institute for Complex Systems (ISC) Consiglio Nazionale delle Ricerche and Physics Department University of Rome, "La Sapienza," Piazzale Aldo Moro, 2, 00185 Roma, Italy
[2]Centro Ricerche Enrico Fermi, Piazza del Viminale, 1, I-00184 Rome, Italy
[3]Max Planck Institute for Chemical Physics of Solids, 01187 Dresden, Germany
[4]Department of Physics, University of Naples Federico II, Via Cintia, Naples 80126, Italy
[5]Terra Quantum AG, Kornhausstrasse 25, CH-9000 St. Gallen, Switzerland
[6]Physics Department, CUNY, City College of City University of New York, 160 Convent Avenue, New York, New York 10031, USA
[7]Leibniz Institute for Solid State and Materials Science Dresden (IFW Dresden), 01069 Dresden, Germany

(Received 9 August 2023; revised 5 December 2023; accepted 7 December 2023; published 5 January 2024)

Van-der-Waals assembly enables the fabrication of novel Josephson junctions featuring an atomically sharp interface between two exfoliated and relatively twisted $Bi_2Sr_2CaCu_2O_{8+x}$ (Bi2212) flakes. In a range of twist angles around 45°, the junction provides a regime where the interlayer two-Cooper pair tunneling dominates the current-phase relation. Here we propose employing this novel junction to realize a capacitively shunted qubit that we call *flowermon*. The *d*-wave nature of the order parameter endows the flowermon with inherent protection against charge-noise-induced relaxation and quasiparticle-induced dissipation. This inherently protected qubit paves the way to a new class of high-coherence hybrid superconducting quantum devices based on unconventional superconductors.

DOI: 10.1103/PhysRevLett.132.017003

One of the most promising ways to achieve a quantum advantage with practical hardware is superconducting quantum circuits. The successful operation of superconducting qubits is based on the robustness of the Josephson effect, which endows the circuit with a lossless nonlinearity [1].

At present, the most commonly used superconducting circuits are based on the transmon qubit [2]. However, the plasmonic nature of the transmon and the macroscopic size of the shunt capacitor plates reduce its coherence time and enhance crosstalk between qubits, posing significant limitations for the implementation of advanced quantum devices comprising a large number of qubits and requiring low error rates [3,4]. As a result, a growing number of works explores alternative designs with inherent protection, such as the rhombus [5–8], fluxonium [9,10], bifluxon [11], blochnium [12], KITE [13,14], $0-\pi$ [15–17], and nanowire-based [18,19] qubits. While significantly higher coherence times are predicted for such circuits in the ideal case, their implementation relies on multiple junctions in a flux loop, making them vulnerable to flux noise and inevitable fabrication imperfections. Here we develop a novel single-junction qubit by integrating a Josephson junction based on the twisted (Van-der-Waals) vdW heterostructure in a transmon architecture that avoids these drawbacks and provides a robust platform for future quantum devices.

Pioneering theoretical [5,20,21] and experimental [22] works proposed to utilize the suppression of tunneling in *d*-wave based Josephson junctions to realize superconducting qubits with an enhanced coherence. These designs also minimized quasiparticle tunneling, highly detrimental for quantum coherence in *d*-wave superconductors. Since a single Cooper-pair tunneling between twisted superconducting *d*-wave islands having different orientations is suppressed due to the momentum mismatch [see Fig. 1(a)], the contribution of the second-harmonic $\cos(2\hat{\varphi})$ of the Josephson energy becomes essential, and the consequent degeneracy of the spectrum can be exploited for creating a decoherence-protected qubit.

One of the ways of obtaining the mismatch was proposed in [23], where using the grain orientation mismatch, the Josephson junctions at grain boundaries of $YBa_2Cu_3O_{7-x}$ with relative granule mismatch angle close to $\pi/4$ demonstrated the degeneracy of the ground state. However, fabrication complexity and the resulting low junction quality hindered the implementation of quantum devices based on grain boundary junctions.

Recent advances in technology allowed one to preserve near-perfect superconductivity and lattice structure in isolated, atomically thin Bi2212 crystals [24–26]. This progress has paved the way for the development of Bi2212-based junctions, through the control of the diffusion of oxygen interstitials—the primary source of detrimental disorder in cuprate Bi2212.

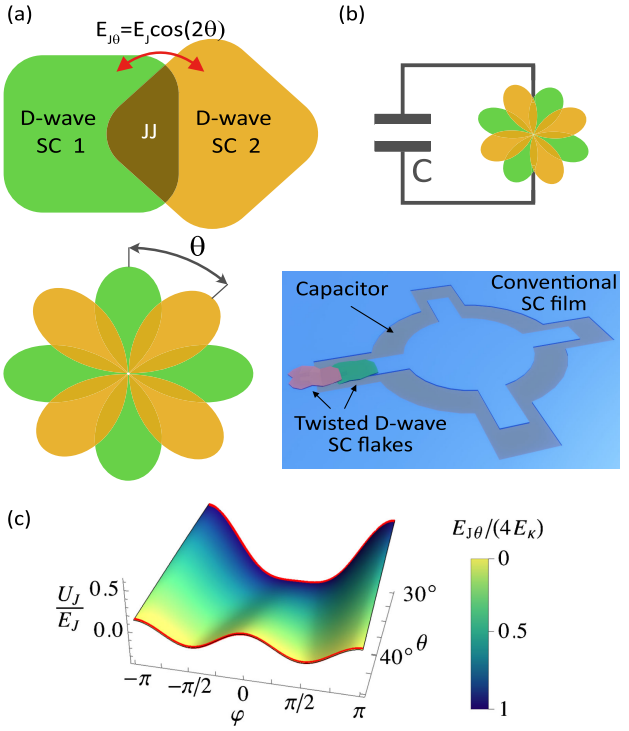

FIG. 1. Potential design for the flowermon qubit. (a) A relative twist of two d-wave flakes placed together to form a Josephson junction can suppress Cooper pair tunneling due to momentum mismatch. At 45° the mismatch completely suppresses single Cooper pair tunneling, and two-pair tunneling dominates the junction. (b) The design of the flowermon with a single d-wave junction shunted by a large capacitor similar to the transmon qubit. The 3D design shows a possible physical implementation with the capacitor pads of a conventional superconductor coupled to the junction. (c) Josephson's potential for different values of the twist angle.

While intrinsic local lattice distortions exist in pristine cuprates [27], they may contribute to a minimal isotropic component that does not impact the d-wave nature of the dominant order parameter. On the other hand, lattice distortions arising from the diffusion of oxygen interstitials are detrimental and must be avoided through engineering the fabrication process. A cryogenic stacking protocol has been devised, leveraging the freezing of oxygen interstitial motion at temperatures well below 200 K (−73 °C) [28,29] and the fast realization of the interface with an average atmosphere of ten part per billion of water molecules. This innovative approach enables the production of high-quality Josephson junctions, revealing a robust dependence of the Josephson energy on the twist angle [30–32].

Here we propose to utilize such a junction as a platform for a novel highly protected qubit that we call *flowermon*. We focus on the simplest design comprising a single capacitively shunted twisted vdW Josephson junction, as sketched in Fig. 1(b). We quantitatively analyze the behavior of the flowermon qubit, highlighting possible decoherence mechanisms for experimentally available parameters, and discuss possible control and measurement schemes.

The dynamics of a Josephson junction are governed by two energy scales: the Josephson's energy E_J, quantifying the energy associated with the tunneling of one Cooper pair across the junction, and the charging energy, E_C, indicating the energy needed to charge the junction with one electron. The Josephson energy is typically related to the junction's critical current as $E_J = I_c\Phi_0/(2\pi)$ where Φ_0 denotes the magnetic flux quantum.

In a junction made of s-wave superconductors the Josephson energy is fixed; therefore the tunneling Hamiltonian can be written as [33]

$$H_J = -E_J\cos(\hat{\varphi}),$$

where $\hat{\varphi}$ denotes the phase difference across the junction. In twisted cuprate nanostructures, the d-wave order parameters of two overlapping superconducting flakes lead to a strong dependence of the Josephson energy on the relative twisting angle θ, $E_{J\theta} = E_J\cos(2\theta)$; see Fig. 1(a). Notice that around $\theta = \pi/4$ $E_{J\theta}$ vanishes, making two-Cooper-pair tunneling, E_κ, the dominant tunneling mechanism, as highlighted in Refs. [34,35] and confirmed experimentally in Ref. [30].

The resulting circuit's Hamiltonian is thus given by

$$H = 4E_C(\hat{n} - n_g)^2 - E_{J\theta}\cos(\hat{\varphi}) + E_\kappa\cos(2\hat{\varphi}), \quad (1)$$

where $\hat{n}$ is the charge conjugate to $\hat{\varphi}$, the gate charge n_g accounts for charge fluctuations induced by external electric fields while the charging energy reads as $E_C = e^2/(2C)$ where C is the capacitance of the shunting capacitor [see Fig. 1(b)] which dominates over the internal junction capacitance. The contribution of higher harmonics beyond the second has been neglected since we consider the limit of weak tunneling. The shape of the Josephson potential, $U_J(\varphi) = -E_{J\theta}\cos(\hat{\varphi}) + E_\kappa\cos(2\hat{\varphi})$ as a function of the twisting angle, is shown in Fig. 1(c). As θ increases from 0 to $\pi/4$, the Josephson potential develops a symmetric double-well structure with two minima at $\varphi = \pm\varphi_0$ with $\varphi_0 = \arccos(E_{J\theta}/4E_\kappa)$ separated by a barrier

$$\Delta U_J = (E_{J\theta} - 4E_\kappa)^2/8E_\kappa. \quad (2)$$

Using Eq. (2), we express the critical angle at which the double-well structure arises as $\theta_c = \frac{1}{2}\arccos(4E_\kappa/E_J)$. The ratio E_κ/E_J thus determines the range of angles in which the qubit can be realized. There is some discrepancy between the theoretical estimates of this ratio [34] as 0.1–0.2, and experimental observations [30] giving 0.02–0.05. Throughout the Letter, we use $E_\kappa/E_J = 0.1$; other values will lead to the renormalization of the operating angles. Note that $E_J \propto \Delta$ and $E_\kappa \propto \Delta^2$; hence high-temperature superconductors such as Bi2212 have a

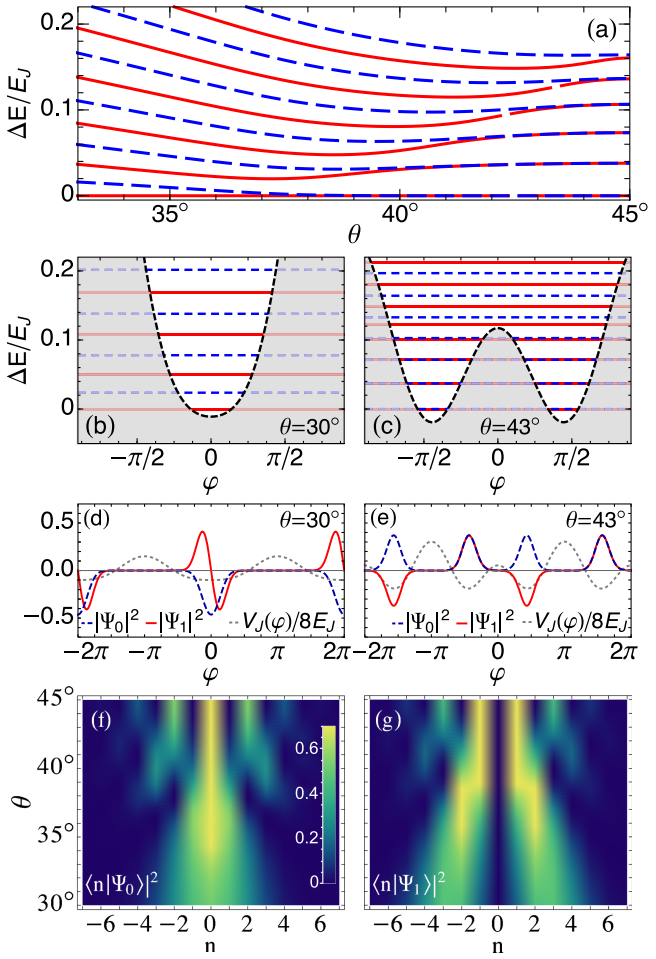

FIG. 2. Flowermon low-energy spectrum. (a) Energy levels of the flowermon qubit as a function of the angle θ. Even and odd levels are shown in red and blue lines respectively; as θ approaches $\pi/4$, the levels combine into quasidegenerate doublets. Here we assume $E_\kappa/E_J = 0.1$ and $E_J/E_C = 2000$. (b),(c) Level structure and potential energy for $\theta = 30°$ and $\theta = 43°$. (d), (e) The wave functions for the ground and first excited state $|\Psi_0\rangle$ and $|\Psi_1\rangle$ in the phase basis for $\theta = 30°$ and $\theta = 43°$. (f),(g) Evolution of the structure of $|\Psi_0\rangle$ and $|\Psi_1\rangle$ in the charge basis as a function of the twisting angle θ.

natural advantage due to higher two-Copper-pair tunneling rates. Additional effects such as inhomogeneity in the twisted junction can further increase E_κ [36]. For further discussion of the relation between junction and qubit parameters, see the Supplemental Material [37].

For $\theta_c < \theta \lesssim \pi/4$ and sufficiently small E_C, the low-energy spectrum reduces to a set of quasidegenerate doublets; see Fig. 2(a). The splitting of each doublet is associated with the tunneling of the phase between the two minima and thus scales exponentially with the ratio $\Delta U_J/E_C$ [13,37]. This transition is shown in Figs. 2(b) and 2(c) where at $\theta = 30°$ the spectrum is quasiharmonic, reminiscent of the spectrum of the transmon qubit, while at $\theta = 43°$ the double well fully develops, and the lowest energy levels are doubly degenerate. In the latter case, the phase is not able to tunnel between two adjacent minima, and, as shown in Fig. 2(e), the corresponding wave functions are localized in two energy wells.

The quasidegeneracy of the levels can be related to the structure of the wave functions in the charge basis. Specifically, at high twisting angles $\theta \gtrsim 40°$, the ground state $|\psi_0\rangle$ contains only even Cooper pair number states, while the first excited state $|\psi_1\rangle$ contains only odd Cooper pair number states; see Figs. 2(f) and 2(g). Eventually, when the angle approaches $\pi/4$, the Josephson energy is completely dominated by double Cooper pair tunneling, and the Cooper pair number parity is conserved. In this limit the wave functions of the even and odd energy levels have a distinct parity in the charge basis.

To illustrate the relevance of the flowermon symmetry properties for qubit protection, we consider the expression of the relaxation rate induced by the capacitive losses estimated using Fermi's golden rule [39]:

$$\Gamma_{1c} = \frac{(8E_C)^2}{\hbar^2} S_{n_g}(\omega_{01}) n_{01}^2, \tag{3}$$

where $n_{xy} = \langle \psi_x | \hat{n} | \psi_y \rangle$ is the matrix element of the charge operator and $S_{n_g}(\omega_{01})$ is the spectral density of the capacitive noise at the qubit operational frequency. Owing to the very small overlap in the charge basis $\hat{n}$ between $|\psi_0\rangle$ and $|\psi_1\rangle$ in the flowermon limit, the corresponding matrix element is exponentially suppressed, preventing energy relaxation; see Fig. 3(b). Looking at twisting angles $\theta \gtrsim 40°$, we, thus, expect an enhancement of the relaxation time over several orders of magnitude as compared with the standard transmon devices which are typically limited by such dielectric losses [40,41].

The corresponding dephasing rate due to charge fluctuations can be approximated within Fermi's golden rule [39] as

$$\Gamma_{\varphi c} \simeq \frac{32E_C^2}{\hbar^2} S_{n_g}(0) |n_{11} - n_{00}|^2, \tag{4}$$

where $S_{n_g}(0)$ is the spectral density of the charge noise at zero frequency. In the case where E_C is sufficiently small with respect to E_J and E_κ, the coefficient $n_{11} - n_{00}$ is exponentially suppressed. The suppression factor can be quantitatively estimated by mapping the Hamiltonian onto a tunneling problem; see the Supplemental Material [37]. Thanks to the large shunt capacitor, the flowermon inherits protection against dephasing induced by the charge noise from the transmon.

In superconducting qubits based on the s-wave junctions, the existence of an energy gap guarantees that the decoherence induced by thermal-equilibrium quasiparticles is exponentially suppressed [42]. Here we show that for sufficiently clean interfaces, an analogous gap behavior is

also present in the flowermon at high twisting angles. To that end, we write the junction Hamiltonian as [34]

$$H = H_{\mathrm{L}} + H_{\mathrm{R}} + H_{\mathrm{T}}, \tag{5}$$

where H_{L} and H_{R} represent the BCS Hamiltonians of the two layers, i.e.,

$$H_{\mathrm{L,R}} = \sum_{\mathbf{k}\sigma} \xi_{\mathbf{k}\mathrm{L,R}} c^{\dagger}_{\mathbf{k}\sigma\mathrm{L,R}} c_{\mathbf{k}\sigma\mathrm{L,R}} + \sum_{\mathbf{k}} \left(\Delta_{\mathbf{k}\mathrm{L,R}} c^{\dagger}_{\mathbf{k}\uparrow\mathrm{L,R}} c^{\dagger}_{-\mathbf{k}\downarrow\mathrm{L,R}} + \mathrm{H.c.} \right), \tag{6}$$

with $c^{\dagger}_{\mathbf{k}\sigma\mathrm{L,R}}$ and $c_{\mathbf{k}\sigma\mathrm{L,R}}$ denoting creation and annihilation operators of electrons with spin σ and momentum $\mathbf{k}$ in layers L and R, while H_{T} represents the interlayer tunneling

$$H_{\mathrm{T}} = \sum_{\mathbf{kp}\sigma} \left(t_{\mathbf{kp}} e^{-i\varphi/2} c^{\dagger}_{\mathbf{k}\sigma\mathrm{L}} c_{\mathbf{p}\sigma\mathrm{R}} + \mathrm{H.c.} \right). \tag{7}$$

The Hamiltonian H thus depends on a small number of parameters, namely, the d-wave gap functions defined as

$$\Delta_{\mathbf{k}\mathrm{L}} = \Delta_d \cos(2\theta_{\mathbf{k}}) \quad \text{and} \quad \Delta_{\mathbf{k}\mathrm{R}} = \Delta_d \cos(2\theta_{\mathbf{k}} - 2\theta), \tag{8}$$

with $\theta_{\mathbf{k}}$ denoting the polar angle in the plane k_x; k_y, the electronic dispersion around the Fermi surface $\xi_{\mathbf{k}} = \hbar^2 k^2/(2m) - \mu$; and the interlayer tunnel amplitude $t_{\mathbf{kp}}$. The latter plays a central role in determining the junction's properties, as discussed in Ref. [43]. Following Refs. [34,44,45], we consider the coherent tunneling limit with the in-plane momentum conservation, $t_{\mathbf{kp}} = t\delta_{\mathbf{k}_{\parallel}\mathbf{p}_{\parallel}}$, suitable to describe weakly disordered c-axis junctions [45]. More accurate microscopic treatment of $t_{\mathbf{kp}}$, including momentum dependence, has been previously considered [46] and can affect the Josephson coupling terms themselves in addition to quasiparticle tunneling [47]. This full treatment is beyond the scope of this Letter and will be the subject of a forthcoming publication.

We calculate the quasiparticle-induced relaxation rate using the approach developed by Refs. [42,48,49], which can be expressed as [37]

$$\Gamma_{\downarrow,\mathrm{qp}} = t^2 |\langle \psi_0 | \sin(\varphi/2) | \psi_1 \rangle|^2 S^{\theta}_{\mathrm{qp}}(\omega_{01}), \tag{9}$$

where $S^{\theta}_{\mathrm{qp}}(\omega_{01})$ is the spectral density of the noise fluctuations induced by quasiparticle tunneling. In the above equation, the θ dependence of the relaxation rate can be traced back to the dependence of both the matrix element $\langle \psi_0 | \sin(\varphi/2) | \psi_1 \rangle$ and spectral density on the twisting angle.

Figure 3(c) shows the results of the numerical calculation of the quasiparticle relaxation rate given by Eq. (9). At high temperatures, high twisting angles correspond to a larger quasiparticle relaxation rate due to the larger prefactor

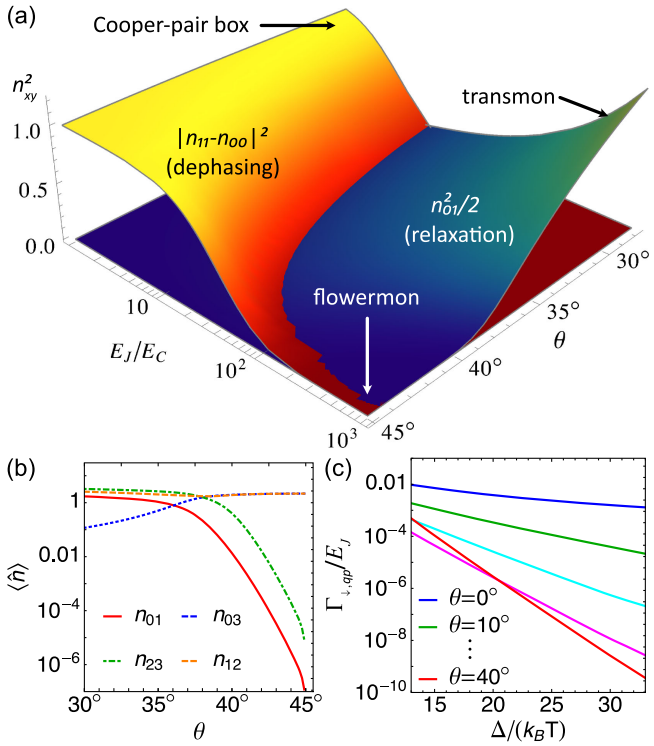

FIG. 3. Protection from decoherence. (a) The charge matrix elements n^2_{01} and $|n_{11} - n_{00}|^2$, related to capacitive relaxation and dephasing rates respectively, plotted vs E_J/E_C and the twisting angle θ. Different regimes are shown, with the flowermon exhibiting protection from both relaxation and dephasing processes. (b) Charge matrix elements n_{01}, n_{03}, n_{23}, and n_{12} vs the twisting angle θ and $E_J/E_C = 2000$. Both n_{01} and n_{23} decay exponentially as $\theta \to 45°$ but with a significant offset. (c) Dependence of the quasiparticle relaxation rate on the ratio Δ/k_BT for different values of the twisting angles ranging between $\theta = 0°$ and $\theta = 40°$.

$\langle \psi_0 | \sin(\varphi/2) | \psi_1 \rangle$. On the contrary, in the low-temperature limit, high twisting angles yield a strong exponential suppression of the quasiparticle rate $\Gamma_{\downarrow,\mathrm{qp}}$, as nodal quasiparticles are forbidden from tunneling due to a momentum mismatch. The numerical results are well fitted by the simple analytical formula, $\Gamma_{\downarrow,\mathrm{qp}} \propto e^{-\Delta_d/(k_BT)\sin(2\theta)^2}$, where, as mentioned above, Δ_d is the d-wave gap in the quasiparticle spectrum at zero twisting angle; this result is reminiscent of what was found in Ref. [44]; see the Supplemental Material [37] for details. This fit indicates that under appropriate conditions the quasiparticles in twisted cuprate vdW heterostructures are effectively gapped, similar to s-wave junctions.

So far we considered only thermal quasiparticles but superconducting devices are often limited by nonequilibrium quasiparticles [50–56]. We expect that the gap behavior highlighted here will similarly protect the flowermon from the decoherence induced by nonequilibrium quasiparticle tunneling [57]. Note that similar protection can be obtained by an s-wave or d-wave Josephson

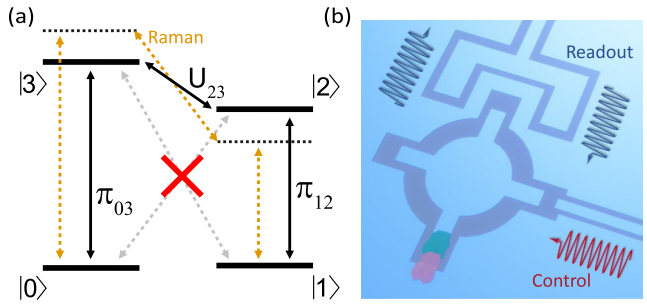

FIG. 4. Manipulation of the flowermon logical states. (a) Logical state manipulation can be performed via the 2nd and 3rd excited states in a regime where the 0-1 matrix element and frequency are near 0, but the amplitude of the $2 \leftrightarrow 3$ transition is still finite. The control is performed by standard microwave π pulses between the 1-2 and 0-3 states, the desired control gate U pulse between the 2-3 states, and again π pulses between the 1-2 and 0-3 states. Alternatively, the 0-1 transition can be driven indirectly by a Raman process via simultaneous off-resonant driving of the 0-3, 2-3, and 2-1 transitions (orange arrows). Note that this protocol works even when $\omega_{01} \to 0$ because the selection rule forbids 0-2 and 1-3 transitions. (b) A sketch of a possible implementation of the device with control and readout lines.

junction [20,58]. Charge density fluctuations or other incoherent fluctuation processes present in cuprate superconductors may provide additional, thermally activated, decoherence mechanisms. These processes are expected to be strongly suppressed at temperatures in the mK range. Nevertheless, studying the quantum dynamics of the flowermon may provide novel tools to probe and understand these processes.

The decoupling of the flowermon qubit from noise sources hampers the direct control and readout of the qubit since the qubit energy $\hbar\omega_{01}$ [see Fig. 2(a)] and the charge matrix element n_{01} [Fig. 3(b)] are exponentially suppressed as $\theta \to 45°$. However, the structure of the flowermon spectrum allows for manipulation through the higher energy levels without sacrificing protection; see Fig. 4(a). Specifically, there is a wide range of angles where the qubit matrix element n_{01} is suppressed while the coupling between the 2nd and 3rd excited states n_{23} is still finite [Fig. 3(b)], e.g., $\theta = 40°$ corresponds to $n_{01} = 0.01$ and $n_{23} = 0.4$. Thus, one can use the excited states for manipulation. For example, a $\pi/2$ pulse in the logical 0-1 space can be performed using standard microwave π pulses between the 1-2 and 0-3 states, a $\pi/2$ pulse between the 2-3 states, and again π pulses between the 1-2 and 0-3 states. To avoid populating the higher states, 0-1 manipulation can also be performed via a simultaneous application of the off-resonant Raman drives through the same energy levels [59]; see the orange line in Fig. 4(a). Note that this scheme works even if ω_{01} is smaller than the frequency selectivity of the control pulses since the transitions 0-2, 1-3 are forbidden by the selection rules $n_{02} = n_{13} = 0$. The higher excited states can be used similarly for measuring the state of the qubit, either by measuring nonprotected transitions such as 0-3, 1-2 directly [60] or through the dispersive coupling of these transitions to a cavity mode [13]. Figure 4(b) shows a possible experimental implementation of such a qubit with the control and readout lines. A more quantitative discussion of this design with realistic qubit parameters is given in [37].

In conclusion, we have developed a qubit design based on a twisted cuprate heterostructure, which we call the flowermon. The simple design of the flowermon, a single junction shunted by a large capacitance similar to that of a transmon, does not require flux tuning or precise control of the fabrication parameters. The d-wave structure of the superconducting phase in this unique junction endows the qubit with physical protection against decoherence. In our Letter, we have discussed the low energy spectrum structure of the qubit at various twist angles and quantitatively analyzed its sensitivity to decoherence mechanisms. Finally, we have presented schemes for the manipulation and readout of this qubit. At twisting angles close to 45°, the flowermon shows exponential suppression of the charge-induced noise, as well as protection from nodal quasiparticle tunneling. The flowermon is thus expected to provide orders of magnitude improvement in the coherence time, promising remarkable progress in future superconducting quantum hardware. Furthermore, the protection offered by the qubit is directly related to the microscopic properties of the cuprate superconductor. Thus, the flowermon promises to become the prototype for a new class of hybrid devices which combine the benefits of quantum materials and coherent quantum circuits, with the possibility of creating superconducting quantum devices which do not require milliKelvin temperatures for their operation.

To build an advantageously practical realization of the flowermon, we have to optimize superconducting galvanic contacts between the deposited circuit and the vdW flake which maintain the circuit coherence [61], and reduce the junction size to obtain higher nonlinearity and operate in the microwave regime. Future devices with multiple qubits can be designed similarly to standard transmon architectures [4], but would require advancing currently available automated vdW fabrication techniques to enable scalable devices [62,63].

The work is partially supported by the Deutsche Forschungsgemeinschaft (DFG 452128813, DFG 512734967, DFG 492704387, and DFG 460444718) and cofunded by the European Union (ERC, cQEDscope, 101075962). The work of V. M. V. is supported by Terra Quantum Inc. and partially by the US NSF Grant No. NSF 1809188 and No. 2105048. The authors are deeply grateful to Shu Yang Frank Zhao, Philip Kim, Bernard van Heck,

Carlo Di Castro, Rosario Fazio, Andrei Zaikin, Kornelius Nielsch, Francesco Tafuri, Giampiero Pepe, Domenico Montemurro, Davide Massarotti, and Pavel A. Volkov for illuminating discussions.

*valentina.brosco@cnr.it
†uri.vool@cpfs.mpg.de

[1] M. H. Devoret and R. J. Schoelkopf, Science **339**, 1169 (2013).
[2] J. Koch, T. M. Yu, J. Gambetta, A. A. Houck, D. I. Schuster, J. Majer, A. Blais, M. H. Devoret, S. M. Girvin, and R. J. Schoelkopf, Phys. Rev. A **76**, 042319 (2007).
[3] M. Brink, J. M. Chow, J. Hertzberg, E. Magesan, and S. Rosenblatt, *Proceedings of the 2018 IEEE International Electron Devices Meeting (IEDM)* (2018), pp. 6.1.1–6.1.3, 10.1109/IEDM.2018.8614500.
[4] F. Arute, K. Arya, R. Babbush, D. Bacon, J. C. Bardin, R. Barends, R. Biswas, S. Boixo, F. G. S. L. Brandao, D. A. Buell *et al.*, Nature (London) **574**, 505 (2019).
[5] G. Blatter, V. B. Geshkenbein, and L. B. Ioffe, Phys. Rev. B **63**, 174511 (2001).
[6] B. Douçot, M. V. Feigel'man, and L. B. Ioffe, Phys. Rev. Lett. **90**, 107003 (2003).
[7] S. Gladchenko, D. Olaya, E. Dupont-Ferrier, B. Douçot, L. B. Ioffe, and M. E. Gershenson, Nat. Phys. **5** (2009).
[8] M. T. Bell, J. Paramanandam, L. B. Ioffe, and M. E. Gershenson, Phys. Rev. Lett. **112**, 167001 (2014).
[9] V. E. Manucharyan, J. Koch, L. I. Glazman, and M. H. Devoret, Science **326**, 113 (2009).
[10] L. B. Nguyen, Y.-H. Lin, A. Somoroff, R. Mencia, N. Grabon, and V. E. Manucharyan, Phys. Rev. X **9**, 041041 (2019).
[11] K. Kalashnikov, W. T. Hsieh, W. Zhang, W.-S. Lu, P. Kamenov, A. Di Paolo, A. Blais, M. E. Gershenson, and M. Bell, PRX Quantum **1**, 010307 (2020).
[12] I. V. Pechenezhskiy, R. A. Mencia, L. B. Nguyen, Y.-H. Lin, and V. E. Manucharyan, Nature (London) **585**, 368 (2020).
[13] W. C. Smith, A. Kou, X. Xiao, U. Vool, and M. H. Devoret, npj Quantum Inf. **6** (2020).
[14] W. C. Smith, M. Villiers, A. Marquet, J. Palomo, M. R. Delbecq, T. Kontos, P. Campagne-Ibarcq, B. Douçot, and Z. Leghtas, Phys. Rev. X **12**, 021002 (2022).
[15] P. Brooks, A. Kitaev, and J. Preskill, Phys. Rev. A **87**, 052306 (2013).
[16] P. Groszkowski, A. D. Paolo, A. L. Grimsmo, A. Blais, D. I. Schuster, A. A. Houck, and J. Koch, New J. Phys. **20**, 043053 (2018).
[17] A. Gyenis, P. S. Mundada, A. Di Paolo, T. M. Hazard, X. You, D. I. Schuster, J. Koch, A. Blais, and A. A. Houck, PRX Quantum **2**, 010339 (2021).
[18] T. W. Larsen, M. E. Gershenson, L. Casparis, A. Kringhøj, N. J. Pearson, R. P. G. McNeil, F. Kuemmeth, P. Krogstrup, K. D. Petersson, and C. M. Marcus, Phys. Rev. Lett. **125**, 056801 (2020).
[19] C. Ciaccia, R. Haller, A. C. C. Drachmann, T. Lindemann, M. J. Manfra, C. Schrade, and C. Schönenberger, arXiv:2306.05467.
[20] L. B. Ioffe, V. B. Geshkenbein, M. V. Feigel'man, A. L. Fauchère, and G. Blatter, Nature (London) **398**, 679 (1999).
[21] A. Blais and A. M. Zagoskin, Phys. Rev. A **61**, 042308 (2000).
[22] T. Bauch, T. Lindström, F. Tafuri, G. Rotoli, P. Delsing, T. Claeson, and F. Lombardi, Science **311**, 57 (2006).
[23] E. Ilichev, M. Grajcar, R. Hlubina, R. P. J. IJsselsteijn, H. E. Hoenig, H.-G. Meyer, A. Golubov, M. H. S. Amin, A. M. Zagoskin, A. N. Omelyanchouk *et al.*, Phys. Rev. Lett. **86**, 5369 (2001).
[24] Y. Yu, L. Ma, P. Cai, R. Zhong, C. Ye, J. Shen, G. D. Gu, X. H. Chen, and Y. Zhang, Nature (London) **575**, 156 (2019).
[25] S. Y. Frank Zhao, N. Poccia, M. G. Panetta, C. Yu, J. W. Johnson, H. Yoo, R. Zhong, G. D. Gu, K. Watanabe, T. Taniguchi, S. V. Postolova, V. M. Vinokur, and P. Kim, Phys. Rev. Lett. **122**, 247001 (2019).
[26] N. Poccia, Shu Yang Frank Zhao, H. Yoo, X. Huang, H. Yan, Y. S. Chu, R. Zhong, G. Gu, C. Mazzoli, K. Watanabe, T. Taniguchi, G. Campi, V. M. Vinokur, and P. Kim, Phys. Rev. Mater. **4**, 114007 (2020).
[27] N. Poccia, A. Ricci, G. Campi, M. Fratini, A. Puri, D. Di Gioacchino, A. Marcelli, M. Reynolds, M. Burghammer, N. L. Saini, G. Aeppli, and A. Bianconi, Proc. Natl. Acad. Sci. U.S.A. **109**, 15685 (2012).
[28] N. Poccia, M. Fratini, A. Ricci, G. Campi, L. Barba, A. Vittorini-Orgeas, G. Bianconi, G. Aeppli, and A. Bianconi, Nat. Mater. **10**, 733 (2011).
[29] M. Fratini, N. Poccia, A. Ricci, G. Campi, M. Burghammer, G. Aeppli, and A. Bianconi, Nature (London) **466**, 841 (2010).
[30] S. Y. F. Zhao, N. Poccia, X. Cui, P. A. Volkov, H. Yoo, R. Engelke, Y. Ronen, R. Zhong, G. Gu, S. Plugge *et al.*, Science **382**, 1422 (2023).
[31] Y. Lee, M. Martini, T. Confalone, S. Shokri, C. N. Saggau, D. Wolf, G. Gu, K. Watanabe, T. Taniguchi, D. Montemurro *et al.*, Adv. Mater. **35**, 2209135 (2023).
[32] M. Martini, Y. Lee, T. Confalone, S. Shokri, C. N. Saggau, D. Wolf, G. Gu, K. Watanabe, T. Taniguchi, D. Montemurro *et al.*, Mater. Today **67**, 106 (2023).
[33] M. Tinkham, *Introduction to Superconductivity* (Dover, New York, 2004).
[34] O. Can, T. Tummuru, R. P. Day, I. Elfimov, A. Damascelli, and M. Franz, Nat. Phys. **17**, 519 (2021).
[35] T. Tummuru, S. Plugge, and M. Franz, Phys. Rev. B **105**, 064501 (2022).
[36] A. C. Yuan, Y. Vituri, E. Berg, B. Spivak, and S. A. Kivelson, Phys. Rev. B **108**, L100505 (2023).
[37] See Supplemental Material at http://link.aps.org/supplemental/10.1103/PhysRevLett.132.017003 for further details on the flowermon's spectrum, quasiparticle relaxation rate and experimentally feasible parameters values, which includes Ref. [38].
[38] K. M. Urwin and F. M. Arscott, Proc. R. Soc. Edinburgh, Sect. A **69**, 28 (1970).
[39] Y. Makhlin, G. Schön, and A. Shnirman, Rev. Mod. Phys. **73**, 357 (2001).
[40] C. Wang, C. Axline, Y. Y. Gao, T. Brecht, Y. Chu, L. Frunzio, M. H. Devoret, and R. J. Schoelkopf, Appl. Phys. Lett. **107**, 162601 (2015).

[41] H. G. Ahmad, V. Brosco, A. Miano, L. Di Palma, M. Arzeo, D. Montemurro, P. Lucignano, G. P. Pepe, F. Tafuri, R. Fazio *et al.*, Phys. Rev. B **105**, 214522 (2022).
[42] G. Catelani, R. J. Schoelkopf, M. H. Devoret, and L. I. Glazman, Phys. Rev. B **84**, 064517 (2011).
[43] R. Haenel, T. Tummuru, and M. Franz, Phys. Rev. B **106**, 104505 (2022).
[44] T. Yokoyama, S. Kawabata, T. Kato, and Y. Tanaka, Phys. Rev. B **76**, 134501 (2007).
[45] C. Bruder, A. van Otterlo, and G. T. Zimanyi, Phys. Rev. B **51**, 12904 (1995).
[46] Y. S. Barash, A. V. Galaktionov, and A. D. Zaikin, Phys. Rev. B **52**, 665 (1995).
[47] X.-Y. Song, Y.-H. Zhang, and A. Vishwanath, Phys. Rev. B **105**, L201102 (2022).
[48] G. Catelani, S. E. Nigg, S. M. Girvin, R. J. Schoelkopf, and L. I. Glazman, Phys. Rev. B **86**, 184514 (2012).
[49] G. Catelani, Phys. Rev. B **89**, 094522 (2014).
[50] J. M. Martinis, M. Ansmann, and J. Aumentado, Phys. Rev. Lett. **103**, 097002 (2009).
[51] P. J. de Visser, D. J. Goldie, P. Diener, S. Withington, J. J. A. Baselmans, and T. M. Klapwijk, Phys. Rev. Lett. **112**, 047004 (2014).
[52] U. Vool, I. M. Pop, K. Sliwa, B. Abdo, C. Wang, T. Brecht, Y. Y. Gao, S. Shankar, M. Hatridge, G. Catelani *et al.*, Phys. Rev. Lett. **113**, 247001 (2014).
[53] C. Wang, Y. Y. Gao, I. M. Pop, U. Vool, C. Axline, T. Brecht, R. W. Heeres, L. Frunzio, M. H. Devoret, G. Catelani *et al.*, Nat. Commun. **5**, 5836 (2014).
[54] K. Serniak, M. Hays, G. de Lange, S. Diamond, S. Shankar, L. D. Burkhart, L. Frunzio, M. Houzet, and M. H. Devoret, Phys. Rev. Lett. **121**, 157701 (2018).
[55] A. P. Vepsäläinen, A. H. Karamlou, J. L. Orrell, A. S. Dogra, B. Loer, F. Vasconcelos, D. K. Kim, A. J. Melville, B. M. Niedzielski, J. L. Yoder *et al.*, Nature (London) **584**, 551 (2020).
[56] L. Cardani, F. Valenti, N. Casali, G. Catelani, T. Charpentier, M. Clemenza, I. Colantoni, A. Cruciani, G. D'Imperio, L. Gironi *et al.*, Nat. Commun. **12**, 2733 (2021).
[57] I. M. Pop, K. Geerlings, G. Catelani, R. J. Schoelkopf, L. I. Glazman, and M. H. Devoret, Nature (London) **508**, 369 (2014).
[58] H. Patel, V. Pathak, O. Can, A. C. Potter, and M. Franz, preceding Letter, Phys. Rev. Lett. **132**, 017002 (2024).
[59] U. Vool, A. Kou, W. C. Smith, N. E. Frattini, K. Serniak, P. Reinhold, I. M. Pop, S. Shankar, L. Frunzio, S. M. Girvin *et al.*, Phys. Rev. Appl. **9**, 054046 (2018).
[60] N. Cottet, H. Xiong, L. B. Nguyen, Y.-H. Lin, and V. E. Manucharyan, Nat. Commun. **12**, 6383 (2021).
[61] C. N. Saggau, Sanaz Shokri, M. Martini, T. Confalone, Y. Lee, D. Wolf, G. Gu, V. Brosco, D. Montemurro, V. M. Vinokur, K. Nielsch, and N. Poccia, ACS Appl. Mater. Interfaces **15**, 51558 (2023).
[62] S. Masubuchi, M. Morimoto, S. Morikawa, M. Onodera, Y. Asakawa, K. Watanabe, T. Taniguchi, and T. Machida, Nat. Commun. **9**, 1413 (2018).
[63] A. J. Mannix, A. Ye, S. H. Sung, A. Ray, F. Mujid, C. Park, M. Lee, J.-H. Kang, R. Shreiner, A. A. High, D. A. Muller, R. Hovden, and J. Park, Nat. Nanotechnol. **17**, 671 (2022).